An improved Synchronous Control Strategy based on Fuzzy controller for PMSM

Shao Jie [1,2], Tan Peng [1,2], Xu Yuan [1,2], Jin Xiangjun [1,2], R. Malekian [3]
[1]*Key Laboratory of Radar Imaging and Microwave Photonics (Nanjing Univ. Aeronaut. Astronaut.), Ministry of Education, College of Electronic and Information Engineering, Nanjing University of Aeronautics and Astronautics, Nanjing, 210016, China*
[2] *Key Laboratory of Underwater Acoustic Signal Processing, Ministry of Education, Southeast University, Nanjing, 210096, China*
[3] *Advanced Sensor Networks Research Group, Department of Electrical, Electronic and Computer Engineering, University of Pretoria, Pretoria, 0002, South Africa*
reza.malekian@ieee.org

***Abstract*—In industry, rail gnawing phenomenon often appears in the synchronous operation of crane. An improved synchronous control strategy for a dual permanent magnet synchronous motor (PMSM) servo system is proposed in this paper. To achieve a synchronous performance with robustness, a cross-coupled synchronous system based on the virtual electronic shaft which both torque and speed are used as feedback signals is developed. Two fuzzy PID compensators with accurate approximation capability based on programmable logic controller (PLC) is implemented to estimate the lumped uncertainty. In the computer simulation, the improved synchronous control strategy is proved to have strong ability to adjust for the external disturbance, and have both smaller convergence time and tracking error. Some experimental results are illustrated to depict the validity of the proposed control approach, which can effectively inhibited wheel's rail gnawing phenomenon in crane.**

***Index Terms*—Permanent Magnet Synchronous Motor, Synchronous Control Strategy, Virtual Shaft, Fuzzy Control.**

I. INTRODUCTION

The permanent magnet synchronous motor (PMSM) has the features of simple structure, high power factor and large moment of inertia. The vector control system of PMSM can achieve high accuracy, robust dynamic performance, and wide range of speed and position control [1]. In *d-q* coordinate system, the vector control method is easier to be realized in PMSM drive systems.

The wheel's slipping, friction, and some out of synchronization in the synchronous operation of motors may conduct rail gnawing in bridge crane. The rail gnawing phenomenon can cause premature failure of wheel rail, seriously affect the operation of a crane, and reduce the service life of equipment. A simple speed control is difficult to meet the requirements of the strong robust operation.

The electrical synchronous control method has been widely used in motor control systems. At present, the electric synchronizations include: parallel control, master-slave control, cross coupling control, and deviation coupling control [2]-[4]. In order to solve the multi-axis synchronous problem, an optimal control method that has both small convergence time and tracking error is necessary, which can quickly and accurately adjust the load torque disturbance [5].

In practical applications, motor parameter variations and load disturbances exist certainly and are unpredictable. Therefore, motors can't achieve precisely synchronization by the parallel control and master-slave control based on open loop control structure. Kulkami did a detailed analysis on the cross coupling compensation method, and put forward the corresponding optimal control scheme [6].

The proportional-integral-derivative (PID) control, neural network control and fuzzy control are the most common control method of motor [7]. In recent years, the particle swarm optimization (PSO) algorithm [8] is also developed. But in some cases, neural network algorithm and PSO algorithm have the problem of huge calculation and poor real-time. The fuzzy control algorithm does not need accurate mathematical model of the controlled object, and is also suitable for nonlinear system. The fuzzy controller has high robustness, and has been widely used in control system.

In this paper, by combining the virtual shaft synchronous control idea with the cross coupling control algorithm, an improved synchronous control strategy is proposed. In the proposed control strategy, the two motors are synchronized with the electronic virtual shaft. Meantime, speed and torque of motors are sent back to the fuzzy PID controller, and are decoupled. When running off track, rail slipping or gnawing happen, the synchronous control system can behave a quick and accurate error correcting capability. Simulation and experimental results show that proposed synchronous control strategy based on PID fuzzy controller has high robustness and strong rail gnawing inhibition

II. PMSM VECTOR CONTROL MODEL

Under the *d-q* rotating coordinate system, the motion

Manuscript received April XX, 20XX; accepted April XX, 20XX.
This research was supported in part by the Foundation of Key Laboratory of China's Education Ministry (UASP1201) and A Project Funded by the Priority Academic Program Development of Jiangsu Higher Education Institutions.

equation and the electromagnet torque equation of PMSM can be described as [9]:

$$J\,\mathrm{d}\omega/\mathrm{d}t = T_e - B\omega - T_L \tag{1}$$

$$T_e = 3p_n\psi_f i_q/2 \tag{2}$$

where J represents total moment inertia of rotor and load, ω is mechanical angular speed, T_e is electromagnetic torque, T_L denotes load torque, B is viscous friction coefficient, i_q, p_n and ψ_f denote the stator current on q axis, permanent flux and number of pole pairs, respectively.

When $i_d = 0$, the voltage and motion equations of PSMS are modified into (3).

$$\begin{bmatrix} \dot{i}_q \\ \dot{\omega} \end{bmatrix} = \begin{bmatrix} -R_s/L_q & -\psi_f/L_q \\ 3p_n\psi_f/2J & -B/J \end{bmatrix} \begin{bmatrix} i_q \\ \omega \end{bmatrix} + \begin{bmatrix} u_q/L_q \\ -T_L/J \end{bmatrix} \tag{3}$$

where u_q is voltage on q axis, R_s is stator resistance.

From (3), both current and speed variables are decoupled. Therefore, controllers about speed and torque can be designed, separately. The control system can be researched as a linear system.

In order to facilitate the simulation research, PMSM's speed control model based on vector control theory has been built up with Simulink toolbox, as shown in Fig. 1.

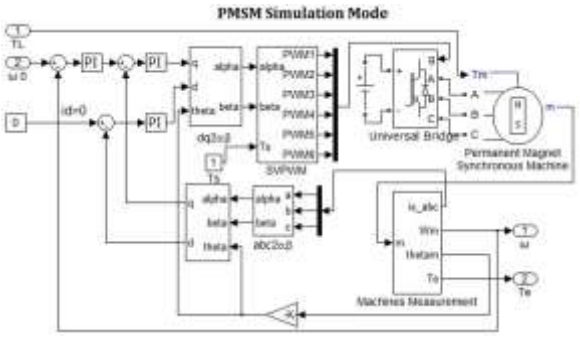

Fig. 1. PMSM's control model base on vector control theory.

III. Synchronous Control Strategy of PMSMs

A. Synchronous Control Strategy Based on Virtual Shaft

The concept of virtual shaft control was originally proposed in [10]. The program is based on the master-slave synchronization, subshaft torque feedback to the principal shaft. Unlike mechanical synchronous method which has fixed parameters, most of the parameters of virtual shaft scheme can be set free in the program. So it has good flexibility, and can also realize a good synchronous control performance by adjusting parameter values continuously.

The traditional electronic virtual shaft scheme can solve the problem of limited load drive. The synchronous control strategy based on electronic virtual shaft is shown in Fig. 2. When a disturbance of torque occurs, the speed of two motors may have significant errors, the motion shafts will likely run off the track.

B. The Improved Synchronous Control Strategy

As a load torque disturbance may damage the synchronous performance of PMSMs, an improved synchronous control strategy based on electronic virtual shaft was proposed, in which a cross coupling loop of speed and load torque was added. As shown in Fig. 3, the two motors are synchronized with speed ω_0 of virtual shaft. The compensation of both $T_A - T_B$ and $\omega_A - \omega_B$ are sent back to the two motors through the compensator. This synchronous system has strong ability to adjust when there is speed and load torque errors between two motors.

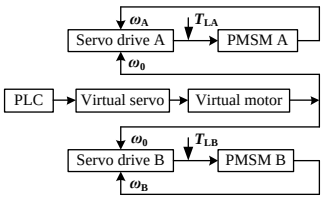

Fig. 2. Synchronous control strategy based on electronic virtual shaft.

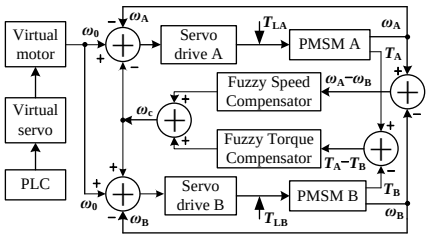

Fig. 3. Improved synchronous control strategy based on virtual shaft.

The outputs of torque compensator are decoupled by Eq. (3), and be used as a correction values of synchronous control system with the output of speed compensator together.

C. The Fuzzy PID Control Algorithm

This design of fuzzy PID controller based on the error $e(k)$ and change of error $ec(k)$ as input. The digital PID control algorithm can be described as follows: [11]

$$\begin{cases} u(k) = u(k-1) + \Delta u(k) \\ \Delta u(k) = k_p(k)ec(k) + k_i(k)e(k) + k_d(k)[ec(k) - ec(k-1)] \end{cases} \tag{5}$$

$$\begin{cases} k_p(k) = k_p(k-1) + \gamma_p \cdot \Delta k_p \\ k_i(k) = k_i(k-1) + \gamma_i \cdot \Delta k_i \\ k_d(k) = k_d(k-1) + \gamma_d \cdot \Delta k_d \end{cases} \tag{6}$$

where γ_p, γ_i, γ_d are correct factors. $u(k)$ and $\Delta u(k)$ is output and change of controller output.

Using fuzzy control toolbox in Matlab, a two-dimensional fuzzy PID controller was built for speed compensation (as shown in Fig. 4).

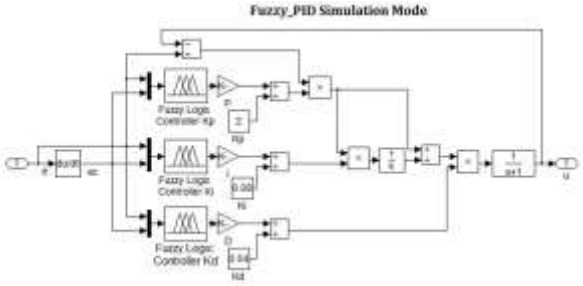

Fig. 4. Fuzzy-PID speed compensator based on Simulink.

Two compensators have the same control structure, except with different parameters. When $\omega_A - \omega_B$ and $T_A - T_B$ are used as inputs of fuzzy PID controller, manipulated variable $u(k)$ is as output of speed or torque compensator. The fuzzy range

of input and output is separated into 7 semantic variables, the fuzzy subsets of input e, ec and Δk_p, Δk_i, Δk_d are defined as $E, EC, \Delta K_p, \Delta K_i, \Delta K_d$ ={NB,NM,NS, ZO,PS,PM,PB}.

The fuzzy inference relationship between input E, EC and output ΔK_p, ΔK_i, ΔK_d are shown in Table I. According to Table I, fuzzy inference outputs can be calculated. The exact amount of the actual parameters of fuzzy PID controller can be obtained by anti-blurring, enabling adjustment of the PID parameters online.

The membership functions of fuzzy variables are shown in Fig. 5. According to the calculated fuzzy quantity, we can choose a kind of judgment method. To adopt centroid defuzzification method, the controlled values will be changed from fuzzy values to accurate values. Table II shows the needed control output values corresponding to the input variables.

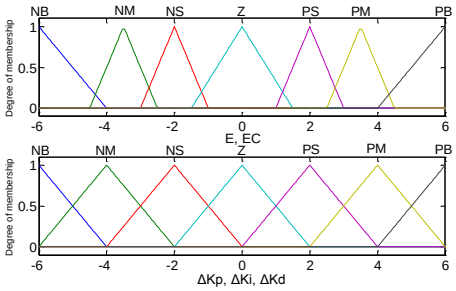

Fig. 5. E, EC, ΔK_p, ΔK_i, ΔK_d membership functions of fuzzy variables.

TABLE I. ΔK_p, ΔK_i, ΔK_d FUZZY RULE BASE.

ΔK_p / ΔK_i/ΔK_d		EC						
		NB	NM	NS	ZO	PS	PM	PB
E	NB	PB/NB/PS	PB/NB/NS	PM/NM/NB	PM/NM/NB	PS/NS/NB	ZO/ZO/NM	ZO/ZO/PS
	NM	PB/NB/PS	PB/NB/NS	PM/NM/NB	PS/NS/NM	PS/NS/NM	ZO/ZO/NS	NS/ZO/ZO
	NS	PM/NB/ZO	PM/NM/NS	PM/NS/NM	PS/NS/NM	ZO/ZO/NS	NS/PS/NS	NS/PS/ZO
	ZO	PM/NM/ZO	PM/NM/NS	PS/NS/NS	ZO/ZO/NS	NS/PS/NS	NM/PM/NS	NM/PM/ZO
	PS	PS/NM/ZO	PS/NS/ZO	ZO/ZO/ZO	NS/PS/ZO	NS/PS/ZO	NM/PM/ZO	NM/PB/ZO
	PM	PS/ZO/PB	ZO/ZO/PS	NS/PS/PS	NM/PS/PS	NM/PM/PS	NM/PB/PS	NB/PB/PB
	PB	ZO/ZO/PB	ZO/ZO/PM	NM/PS/PM	NM/PM/PM	NM/PM/PS	NB/PB/PS	NB/PB/PB

TABLE II. ΔK_p, ΔK_i, ΔK_d FUZZY CONTROL LOOKUP TABLE.

ΔK_p / ΔK_i/ΔK_d		EC						
		NB	NM	NS	ZO	PS	PM	PB
E	NB	5.4/-5.4/2	5.4/-5.4/-2	4/-4/-5.4	4/-4/-5.4	2/-2/-5.4	0/0/-4	0/0/2
	NM	5.4/-5.4/2	5.4/-5.4/-2	4/-4/-5.4	2/-2/-4	2/-2/-4	0/0/-2	-2/0/0
	NS	4/-5.4/0	4/-4/-2	4/-2/-4	2/-2/-4	0/0/-2	-2/2/-2	-2/2/0
	ZO	4/-4/0	4/-4/-2	2/-2/-2	0/0/-2	-2/2/-2	-4/4/-2	-4/4/0
	PS	2/-4/0	2/-2/0	0/0/0	-2/2/0	-2/2/0	-4/4/0	-4/5.4/0
	PM	2/0/5.4	0/0/2	-2/2/2	-4/2/2	-4/4/2	-4/5.4/2	-5.4/5.4/5.4
	PB	0/0/5.4	0/0/4	-4/2/4	-4/4/4	-4/4/2	-5.4/5.4/2	-5.4/5.4/5.4

In the actual system, the speed is recorded by the number of pulses (bits width of the encoder is 20). For speed compensator, set $e_\omega = (\omega_A - \omega_B) \in$ [-40000, 40000], $ec_\omega \in$ [-120000, 120000]. The design method of torque compensator is similar. Based on experimental data, set $e_T = (T_A - T_B) \in$ [-200, 200] (Torque output of PMSM is expressed as a percentage of rated torque), $ec_T \in$[-255, 255]. The membership function of the speed cross-coupling compensator and torque compensator can be designed [12].

The fuzzy-PID controllers have been realized by PLC programming.

IV. SIMULATION RESULTS AND ANALYSIS

By using the Matlab toolboxes of power system and fuzzy logic system, a model of PMSM synchronous system is built, and the parameters are listed in Table III. The initial values of speed compensator are $k_p(0)=2$, $k_i(0)=0.08$, $k_d(0)=0.04$, $\Delta k_p \in [-0.5,0.5]$, $\Delta k_i \in [-0.3,0.3]$, $\Delta k_d \in [-0.01,0.01]$, $\gamma_p = 0.083$, $\gamma_i = 0.05$, $\gamma_d = 0.0017$.

In the simulation experiment, as showed in Fig. 6, some disturbances are added into the load torque artificially. The initial load torque value of virtual shaft is 10N•m. At 0.6s the load torque of shaft B suddenly increases to 12N•m and it returns to 10N•m at 0.63s. At 1.2s the load torque of shaft A suddenly decreases to 8N•m and it returns to 10N•m at 1.3s. Since the load torque changes, the speed responses of shaft A and shaft B will change accordingly.

TABLE III. THE PARAMETERS OF USED PMSM.

Item	Value
Voltage (V)	380
Power (kW)	4
torque (N•m)	0.783
Stator resistance (Ω)	0.432
L_{md} (H)	0.007
J ($\times 10^{-4}$kg•m^2)	1414
p_n	2

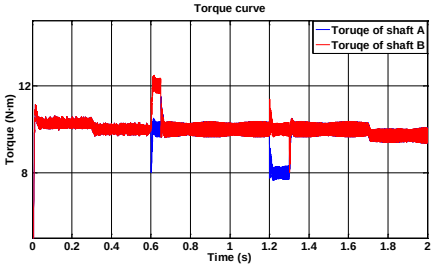

Fig. 6. Simulated torque curves of the shafts.

The synchronous control model is simulated under three different control strategies. The first control strategy only has the speed feedback control and works under the traditional PID control algorithm (Case 1). The second one has a

double-feedback compensation of speed and load torque under the traditional PID control algorithm (Case 2). The third control strategy has the double-feedback compensation using the fuzzy PID controller (Case 3). The simulation results of speed response under three control strategies are showed in Fig. 7. The parameters k_p , k_i , k_d of speed compensator under Case 3 are showed in Fig. 8. Table IV summarizes the comparisons of control performance about three control strategies with respect to the simulation results.

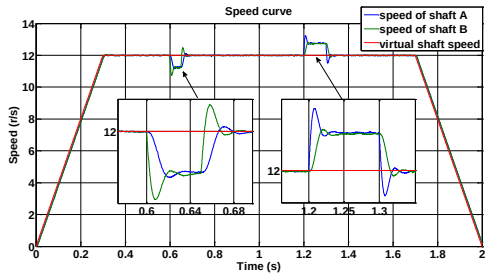

(a) Case 1

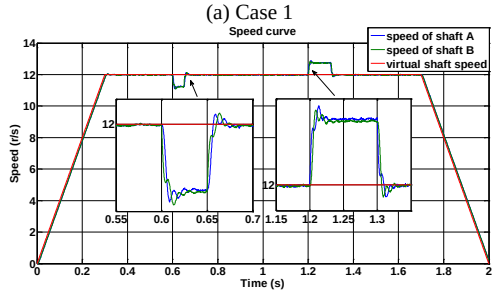

(b) Case 2

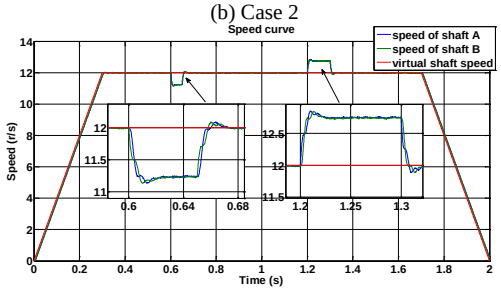

(c) Case 3

Fig. 7. Simulated speed curves.

From Fig. 7 and Table IV, it can be seen that the speed response of Case 1 has the largest overshoot which is up to 66% and the longest setting time of 0.07s. Comparing to Case 1, the overshoot of speed response under Case 2 is decreased to 38.4% and the setting time is reduced to 0.06s. The speed response of Case 2 is faster and more stable than Case 1. Under Case 3, the overshoot is only 13.3%, the setting time is just 0.02s, and the speed response curves of shaft A and shaft B are the smoothest. The method of the Case 3 is more flexible and has better adaptability, so the synchronous performance is the best about three control strategies. As listed in Table IV, the maximum error, the average error and the standard deviation of speed between shaft A and virtual shaft (ω_A - ω_0), shaft B and virtual shaft (ω_B - ω_0), shaft A and shaft B (ω_A - ω_B) are the smallest under Case 3. Both the speed curves and the comparisons of simulation results in TABLE IV show that when the load torque of shaft A or shaft B changes, the improved synchronous control strategy (Case 3) has greatly decreased the overshoot and the setting time of speed response, it can get a very good synchronization.

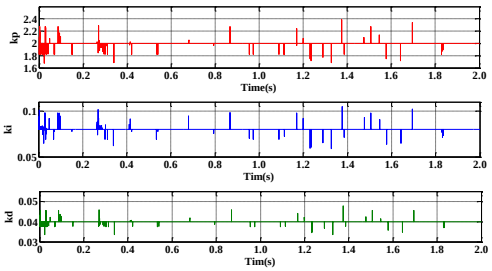

Fig. 8. Parameters k_p , k_i , k_d of speed compensator.

TABLE IV. COMPARISONS OF SIMULATION RESULTS.

Index		Case 1	Case 2	Case 3
Overshoot		66%	38.4%	13.3%
Setting Time (s)		0.07	0.06	0.02
Max. Error (r/s)	ω_A-ω_0	1.1470	0.8870	0.7865
	ω_B-ω_0	1.2487	0.9223	0.7151
	ω_A-ω_B	1.0570	0.4446	0.4153
Average Error (r/s)	ω_A-ω_0	0.3312	0.2111	0.2112
	ω_B-ω_0	0.3236	0.2538	0.2258
	ω_A-ω_B	0.0823	0.0427	0.0054
Standard Deviation (r^2/s^2)	ω_A-ω_0	2.5689	2.1607	1.5063
	ω_B-ω_0	2.5370	2.2405	1.4381
	ω_A-ω_B	1.4150	0.5398	0.3398

V. EXPERIMENTAL RESULTS AND ANALYSIS

In some radioactive material warehouse, it is necessary to ensure workers safety and avoid radiation. An intelligent remote crane system which can work efficiently and safely in an unmanned environment has been designed. The engineering scene is showed in Fig. 9.

Fig. 9. The experimental scene.

This crane which is a control system based on visual servo technology can accurately deposit and withdraw the objects in storage well. In order to meet the requirements of positioning accuracy (within ±5mm), the crane motors must have good performance of dynamic synchronization.

In practical engineering, the electrical parameters of selected PMSM are listed in Table V. The operating data of motors based on different control strategies is read out from PLC. The torque curves and speed curves which can reflect system's synchronous performance are drawn by Matlab.

TABLE V. OVERHEAD CRANE MOTOR PARAMETERS.

Item	Value
Voltage (V)	200
Power (kW)	1.8
Torque (N•m)	11.5
Current (A)	16.7
Speed (min^{-1})	1500
Torque constant (N•m)	0.748
Moment of inertia ($\times 10^{-4}$kg•m^2)	28.1
Power change rate (kW/s)	47.1

In the condition that the trolley-load system is located in the

middle of crane beams, the torque curves and speed curves are shown in Fig. 10 and Fig.11, respectively. Torque curves in Fig. 10(a) are under Case 1, the torque of shaft A and shaft B are seriously asymmetric. When running to 16s, the motor's torque of shaft B increases rapidly, and has reached 100% of the rated torque at 19s due to external disturbances. After the motor of shaft B running with the rated torque for a few seconds, the motor will alarm at 23s. Torque curves in Fig. 10(b) are under Case 3. Different to Case 1, the torque of two shafts under Case 3 has good symmetry, and the stress of two motor wheels is balanced. The synchronization performance under the Case 3 is much better than the Case 1.

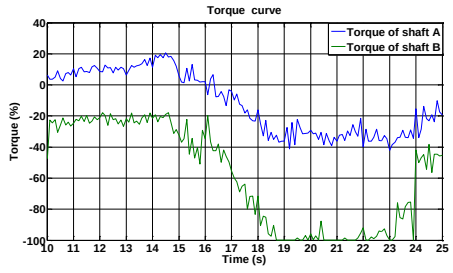

(a) Case 1

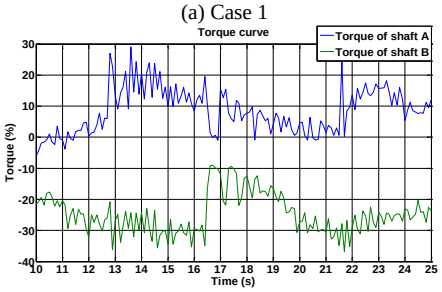

(b) Case 3

Fig. 10. Experimental torque curves when the trolley-load system is located in the middle of crane beams.

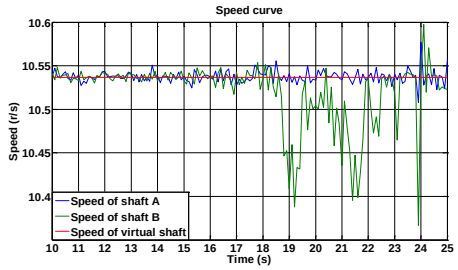

(a) Case 1

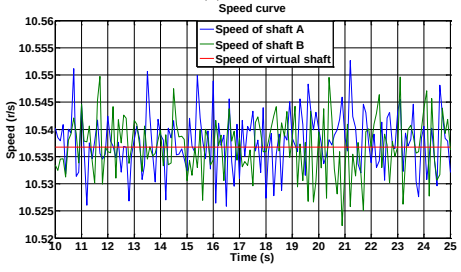

(b) Case 3

Fig. 11. Experimental speed curves when the trolley-load system is located in the middle of crane beams.

The speed curves in Fig. 11(a) are under Case 1. When the torque of shaft B suddenly changes at 16s, the speed of shaft B's motor generates a great deviation, during time 18s~24s, the speed response of shaft B is very unstable since the torque is 100% of the rated torque, and the maximum fluctuation of speed is up to 0.23r/s. Under Case 1, the system can't adjust the speed of two motors to reach equilibrium timely. The speed curves in Fig. 11(b) are under Case 3. Using the speed-torque feedback compensation with the fuzzy PID controller, the system can adjust the speed of two motors immediately, the maximum fluctuation of speed is only 0.02r/s, this synchronous control strategy has strong stability and robustness, and the response is very fast.

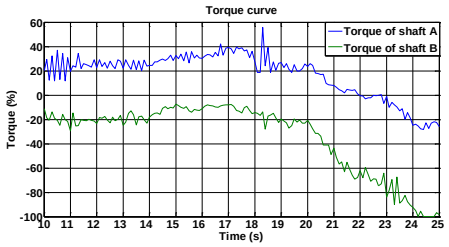

(a) Case 1 (the trolley-load in the left location)

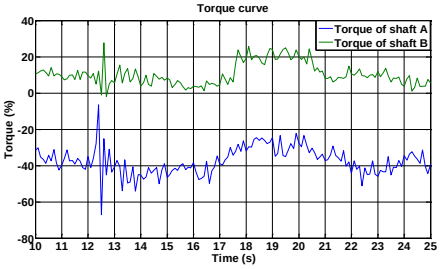

(b) Case 3 (the trolley-load in the left location)

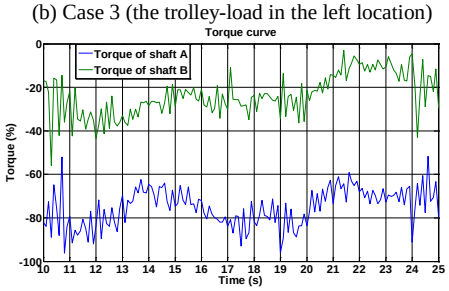

(c) Case 1 (the trolley-load in the right location)

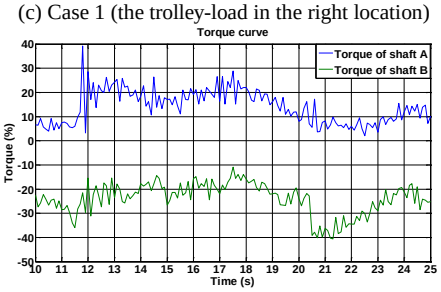

(d) Case 3 (the trolley-load in the right location)

Fig. 12. Experimental torque curves when the trolley-load system is located in the left and right side of crane beams.

TABLE VI. COMPARISONS OF EXPERIMENTAL RESULTS.

Control strategy	**Performance**		**Load location**		
			middle	left	right
Case 1	Max. Error	ω_A-ω_0	0.0408	0.0218	0.1220
		ω_B-ω_0	0.1697	0.1020	0.0624
	Average Error	ω_A-ω_0	0.0052	0.0050	0.0089
		ω_B-ω_0	0.0213	0.0066	0.0083
	Standard Deviation	ω_A-ω_0	0.007	0.007	0.020
		ω_A-ω_0	0.040	0.010	0.010
Case 3	Max. Error	ω_A-ω_0	0.0159	0.0171	0.0179
		ω_B-ω_0	0.0144	0.0141	0.0151
	Average Error	ω_A-ω_0	0.0042	0.0042	0.0050
		ω_B-ω_0	0.0042	0.0048	0.0045
	Standard Deviation	ω_A-ω_0	0.005	0.005	0.006
		ω_A-ω_0	0.005	0.006	0.006

When trolley-load system is located in the middle of the

crane beams, the two PMSMs of overhead crane would bear a same load. In the opposite, when it is located in the left or the right of the crane beam, the overhead crane's motors would bear an unbalanced load, and their torque curves are shown in Fig. 12. Table VI summarizes the comparisons of control performance under Case 1 and Case 3 with respect to the experimental results when the trolley-load system is located in the middle, left and right side of the crane beam.

When the trolley-load system is located in the left side of the crane beam, as shown in Fig. 12(a), the torque curves under Case 1 start to decline at 8s and the torque of shaft B drops to 100% of the rated torque at about 14s, the motor of shaft B can't work normally and will alarm. When the trolley-load system is located in the right side of the crane beam, as shown in Fig. 12(c), the torque of two shafts under Case 1 are both negative, the motor of shaft B is dragging the motor of shaft A, which is a wrong way of running. It can be seen from Fig. 10(b), Fig. 12(b) and Fig. 12(d) that under Case 3, no matter where the trolley-load system is located, the torque of two shafts always has good symmetry, and the direction of two motors are opposite, means that the system is working correctly and has good synchronization. As listed in Table VI, the same kind of deviations under Case 3 are all smaller than the errors under Case 1, it also prove that no matter where the trolley-load system is located, Case 3 has much better synchronization performance than Case 1.

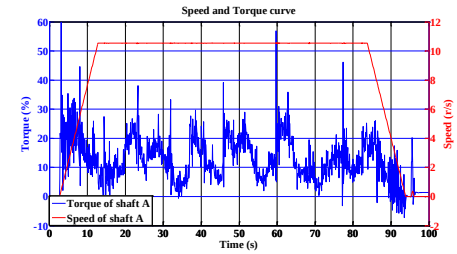

(a) Speed and torque of shaft A.

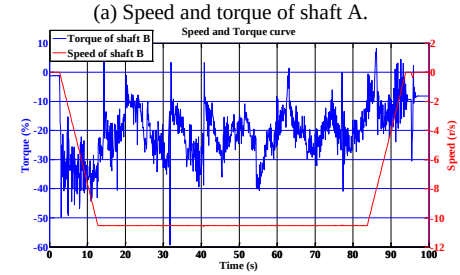

(b) Speed and torque of shaft B.

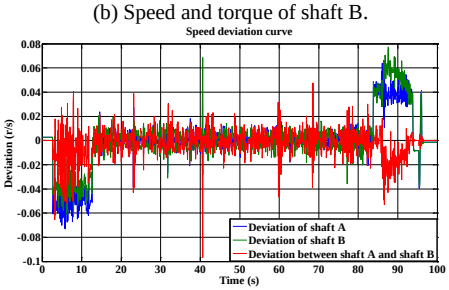

(c) Speed deviation.

Fig. 13. Complete positioning motion curves.

In a complete positioning motion of the crane, the speed curves, the torque curves and the speed deviation curves of two motors are shown in Fig. 13.

It can be seen from Fig. 13(a) and Fig. 13(b) that the torque and speed of shaft A and shaft B are symmetrical, and both the torque variations are maintained below 60% of the rated torque, the motors are running synchronously and stably. Fig. 13(c) shows the speed deviation of two shafts. During the accelerated startup process and the decelerated stop process, the speed deviation of two shafts is larger. But when the crane is running at a constant speed, the average speed deviation between two motors remains at about 0.02r/s, the motors has achieved synchronization. Proposed synchronous control strategy can effectively avoid the gnawing rail phenomenon.

VI. Conclusions

In bridge crane operation, the rail gnawing is a serious problem. In this paper, an improved synchronous control strategy is proposed. A cross-coupled synchronous system based on the virtual electronic shaft which both torque and speed are used as feedback signals is developed. In this approach, two fuzzy PID compensators with accurate approximation capability based on PLC are implemented to estimate the lumped uncertainty. The results of simulation and experiment show that the proposed synchronous control strategy has the advantages in strong robustness, a good dynamic performance, and rapid response. The engineering application results also proved that developed PMSM's synchronous system can achieve a better control result, and enhance the ability of inhibiting rail gnawing greatly.

References

[1] Underwood S. J., Husain I., "Online parameter estimation and adaptive control of permanent-magnet synchronous machines," *IEEE Trans. Industrial Electronics*, vol. 57, no. 7, pp. 2435-2443, Jul. 2010.

[2] Lin F.-J., Hsieh H.-J., Chou P.-H., Lin Y.-S., "Digital signal processor-based cross-coupled synchronous control of dual linear motors via functional link radial basis function network," *IET Control Theory and Applications*, vol. 5, no. 4, pp. 552-564, Mar. 2011.

[3] Lin F.-J., Chou P.-H., Chen C.-S., Lin Y.-S., "DSP-based cross-coupled synchronous control for dual linear motors via intelligent complementary sliding mode control," *IEEE Trans. Industrial Electronics*, vol. 59, no. 2, pp. 1061-1073, Feb. 2012.

[4] Cheng M. H.-M., Mitra A., Chen C. Y., "Synchronization controller synthesis of multi-axis motion system," *in Proc. 4th ICICIC*, pp. 918-921, Dec. 2009.

[5] Wang Z., Zheng Y., Zou Z. X., Cheng M., "Position Sensorless Control of Interleaved CSI Fed PMSM Drive With Extended Kalman Filter," *IEEE Trans. Magnetics*, vol. 48, no. 11, pp. 3688-3691, Nov. 2012.

[6] Kulkami P. K., Srinivasan K., "Optimal contouring control of multiaxial feed drive servo mechanisms", *ASME J. Eng. Ind.*, vol. 111, no.2, pp.140-148, May 1989

[7] Rubaai A., Castro-Sitiriche M. J., Ofoli A. R., "DSP-Based Laboratory Implementation of Hybrid Fuzzy-PID Controller Using Genetic Optimization for High-Performance Motor Drives," *IEEE Trans. Industry Applications*, vol. 44, no. 6, pp.1977-1986, Nov. 2008..

[8] Huang M. M., Lin H., Huang Y. K., Jin P., Guo Y. J., "Fuzzy Control for Flux Weakening of Hybrid Exciting Synchronous Motor Based on Particle Swarm Optimization Algorithm," *IEEE Trans. Magnetics*, vol. 48, no. 11, pp. 2989-2992, Nov. 2012.

[9] Wai R.-J., Chuang K.-L., Lee J.-D., "On-Line Supervisory Control Design for Maglev Transportation System via Total Sliding-Mode Approach and Particle Swarm Optimization," *IEEE Trans. Automatic Control*, vol.55, no.7, pp.1544-1559, July 2010.

[10] Lorenz R. D., Schmidt P. B., "Synchronized motion control for process automation," *in Rec. IEEE Industry Applications Society Annual Meeting*, vol.2, pp.1693-1698, 1989

[11] Feng G., "A Survey on Analysis and Design of Model-Based Fuzzy Control Systems," *IEEE Trans. Fuzzy Systems*, vol.14, no.5, pp. 676-697, Oct. 2006.

[12] Xia C. L., Guo C., Shi T. N. "A neural-network-identifier and fuzzy-controller-based algorithm for dynamic decoupling control of permanent-magnet spherical motor," *IEEE Trans. Ind. Electron.*, vol.57, no.8, pp. 2868-2878, Aug. 2010.